

**ABRASIVE WATER JET CUTTING (AWJC) OF CO-CR-MO ALLOY
INVESTMENT CASTINGS IN THE MEDICAL DEVICE INDUSTRY**

M. Cashman, S. Ramirez
DePuy (Ireland)
Cork, Ireland

S.L. Soo, D.E.T. Shepherd
University of Birmingham
Birmingham, UK

A. Rabani
University of Nottingham
Nottingham, UK

ABSTRACT

Investment castings (usually involving ceramic based shells) have traditionally been separated from the mould tree using an abrasive cutting operation. While material removal rates are relatively high, the process unfortunately suffers from poor accuracy control that often necessitates further finishing operations. Following an overview of key considerations in investment casting including tree configurations and gate profile, the paper details experimental work to investigate the feasibility of abrasive waterjet cutting (AWJC) as an alternative to grinding for component cut-off. The workpiece material was a high strength cobalt-chromium-molybdenum alloy (ASTM F-75) commonly used for orthopaedic implants. Preferred AWJC cutting parameters were established for material thicknesses up to 30 mm. Specimens of 13 mm and 30 mm thickness were cut through at maximum traverse speeds of 220 mm/min and 80 mm/min respectively. Abrasive grit embedment was observed primarily at the top surface and exit region of the cut. The effect of investment casting refractory shells on the AWJC process was examined. In addition, a comparative analysis of performance and cost with alternative cutting methods was also performed.

1. INTRODUCTION

ASTM F-75 is a cobalt-chromium-molybdenum (CoCrMo) alloy commonly used for orthopaedic implants. These medical devices require high wear resistance and the ability to withstand complex loading conditions for long-term periods (>20 years) in a corrosive environment. Metals such as CoCrMo, titanium and its alloys, and certain austenitic stainless steels are suited for use in orthopaedic implants due to their high strength and exhibition of favourable corrosion resistance *in vivo*.

The investment casting process is used to manufacture small-medium size components including medical devices (e.g. orthopaedic implants), aerospace components (e.g. turbine blades), and automotive components. It can produce complex shapes that would be difficult or impossible with die casting. The process starts with injection of a wax pattern into a metal mould. Multiple patterns are assembled onto a wax downsprue to form a wax tree. The downsprue and routes into the patterns (“gates”) are called the runner system. The wax tree is coated in a ceramic shell until the desired shell thickness is achieved. The wax is melted out and the shell is fired in an oven before molten metal is poured in to form the cast tree. After cooling, the refractory is removed by vibration, waterjets, blasting, or cavitation cleaning. The castings are cut from the runner system, normally by abrasive wheel. If necessary, further processing obtains the desired surface finish, e.g. blasting, grinding or polishing.

Abrasive waterjet cutting (AWJC) is an alternative cutting process that may be suitable for runner system removal of investment castings. A high-pressure pump (up to 775 MPa) is used to guide a narrow waterjet entrained with abrasive media through a nozzle to cut almost any material. AWJC can produce parts quickly, with high tolerances, and minimal fixturing.

Runner system design and gate profile are key considerations for the quality of castings produced. Some of the key considerations pertaining to AWJC are as follows:

- The tree must be configured in such a manner that the abrasive jet exit does not impinge on parts below.
- There must be sufficient access to the cutting area. Runner system removal with abrasive wheel requires a minimal access path just greater than the width of the cutting blade (<10 mm).
- The runner system and gates must be thick enough to allow the castings to fill before the gate solidifies. AWJC speed significantly reduces with increasing material thickness.
- Five-axis cutting capability may be required, particularly for additional runner system components. These are often added to aid wax melt-out or to provide strength to the casting.
- Symmetrical tree designs and rounded gates contribute to smoother flow into the patterns. The cast tree design may be prohibitively restrictive on AWJ cutting head geometry.

The research aims to determine the cutting speeds and associated AWJC parameters required for cutting through various thicknesses of CoCrMo investment castings.

2. WORKPIECE MATERIAL, EQUIPMENT AND EXPERIMENTAL PROCEDURES

The cut material was a cobalt-chromium-molybdenum alloy (ASTM F-75). The nonferrous alloy is favoured for use in biomedical devices due to its high strength and biocompatibility. The chemical composition and mechanical properties are given in tables 1 and 2 respectively (ASTM).

Table 1 Chemical composition of ASTM F-75

Element	ASTM F-75
Cobalt, Co	Balance
Chromium, Cr	27-30
Molybdenum, Mo	5-7
Nickel, Ni	<0.5
Iron, Fe	<0.75
Carbon, C	<0.35
Silicone, Si	<1
Manganese, Mn	<1
Tungsten, W	<0.2
Phosphorus, P	<0.02
Sulphur, S	<0.01
Nitrogen, N	<0.25
Aluminium, Al	<0.1
Titanium, Ti	<0.1
Boron, B	<0.01

Table 2 Mechanical properties of CoCrMo alloy

Property	ASTM F75 required	As cast CoCrMo (Cawley et al.)
Elongation at break (%)	>8%	11
0.2% Proof Strength (MPa)	450 MPa	510
Ultimate Tensile Strength (MPa)	655 MPa	926
Hardness (H_V)		310
Elastic modulus (GPa)		210
Density ($\times 1000 \text{ kg/m}^3$)		8

The test specimens were CoCrMo investment castings produced in DePuy, Ireland. The cylindrical specimens were 30 ± 1.5 mm diameter (figure 1(i)). The flat specimens were 37 x 140 mm with a thickness of 13 ± 1 (figure 1(ii)), and 40 x 40 mm with a thickness of 26.9 ± 1 mm. Cuts were made at approx. 5 mm intervals. To evaluate the effect that a refractory coating may have on cutting efficiency, an aluminosilicate refractory of 6 mm thickness was fixed to the surface of a 13 mm thick plate (figure 1(iii)). The standoff distance was adjusted to 3 mm above the ceramic material.



Figure 1 Test specimens prior to cutting (i) 30 mm diameter cylinder (ii) 13 mm thick plate (iii) refractory coated specimen

Abrasive waterjet cutting trials were performed with an Ormond 5-axis AWJ cutting system at the University of Nottingham, UK (Figure 2). The UHP pump used was a KMT streamline SL-V100D capable of providing maximum water pressure of 413.7 MPa (60,000 psi). The nozzle consisted of a sapphire orifice of diameter 0.3 mm and a focusing tube of diameter 1.06 mm. GMA 80-grit garnet abrasive was used.

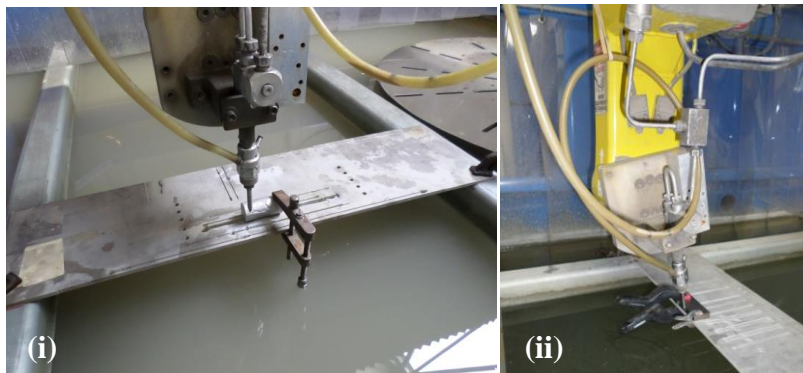


Figure 2 AWJC experimental setup (i) Cylindrical specimens, (ii) Flat specimens (cutting head tilted to 102°)

The ranges of parameters tested are given in table 3 below.

Table 3 Process parameters

Pressure, p (MPa)	345
Abrasive Mass Flow rate, m_a (g/min)	145, 300, 490
Standoff distance, s (mm)	3
Traverse Speed, V_t (mm/min)	36 - 400
Jet impingement angle, θ (°)	90, 102

The traverse speed and jet impingement angle were CNC controlled. The standoff distance was measured with a 3 mm gauge. The standoff distance for the cylindrical samples was measured at the top of the samples with the gauge plate at 90° to the cutting head. The abrasive mass was measured on electronic scales after allowing the abrasive to flow freely for one minute.

In order to analyze the cut face of all specimens, wire-EDM (Electrical Discharge Machining) at the University of Birmingham, UK, was used to separate any specimens that were not entirely cut through with the abrasive waterjet. The depth of cut, striation angles and surface roughness

were used to determine the cut quality, with the primary objective of maximizing V_t . The minimum depth of cut for the cylindrical specimens was measured parallel from the top of the cut face. Surface roughness was measured in the direction of jet traverse using a surface profilometer (Form Talysurf 120L) at the University of Birmingham, UK. The cut off and traverse length were 0.8 mm and 4.0 mm respectively. Four measurements were made at each of the following depths through the cut: 1.5, 7 and 11.5 mm. ImageJ software was used to calculate the Declination Angle (DA) at the exit of the cut. The images were rotated so that the bottom edge of the specimen was parallel with the image edge. Ten lines were drawn to coincide with prominent striation angles at the jet exit and the line angles were recorded (figure 3). Scanning Electron Microscopy (SEM) was used to study the microstructure of the machined specimens.

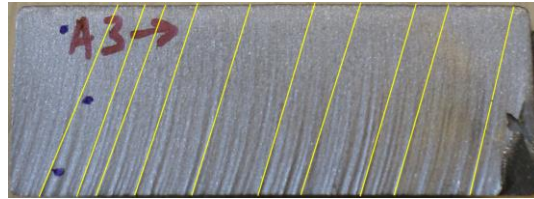


Figure 3 Measurement of Declination Angle (DA) using ImageJ

3. RESULTS AND DISCUSSION

3.1 Material Removal in CoCrMo Alloy

Material density has been used by Hlavac *et al.* (2009) as a parameter to predict AWJC quality of different materials. CoCrMo has a density similar to that of stainless steel ($8 \times 1000 \text{ kg/m}^3$) and material removal occurs in a similar manner by “microchip formation, ploughing and rubbing” (Arola). The predominant mechanism depends on the angle of abrasive impingement and the material properties. Microchip formation occurs primarily in the IDR where the angle of abrasive impact is high. A rounded edge occurs at the top of the cut (figure 4).

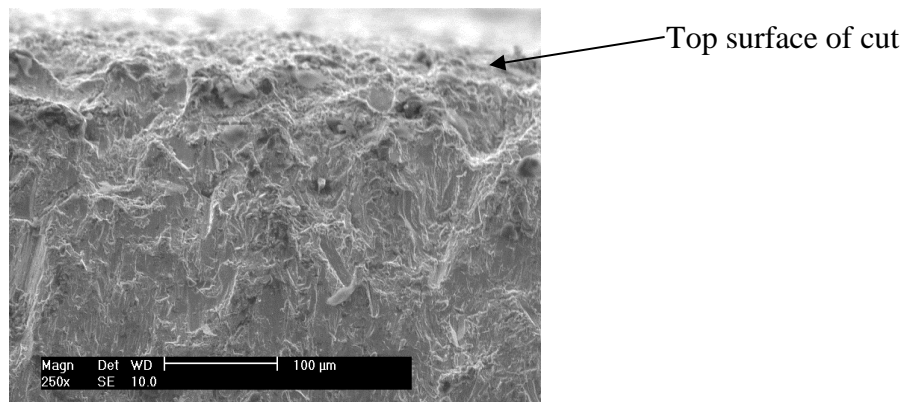


Figure 4 SEM image of Initial Damage Region (IDR)

At lower impact angles, deformation wear by the abrasive (ploughing and rubbing) removes material in the SCR and RCR (figure 5).

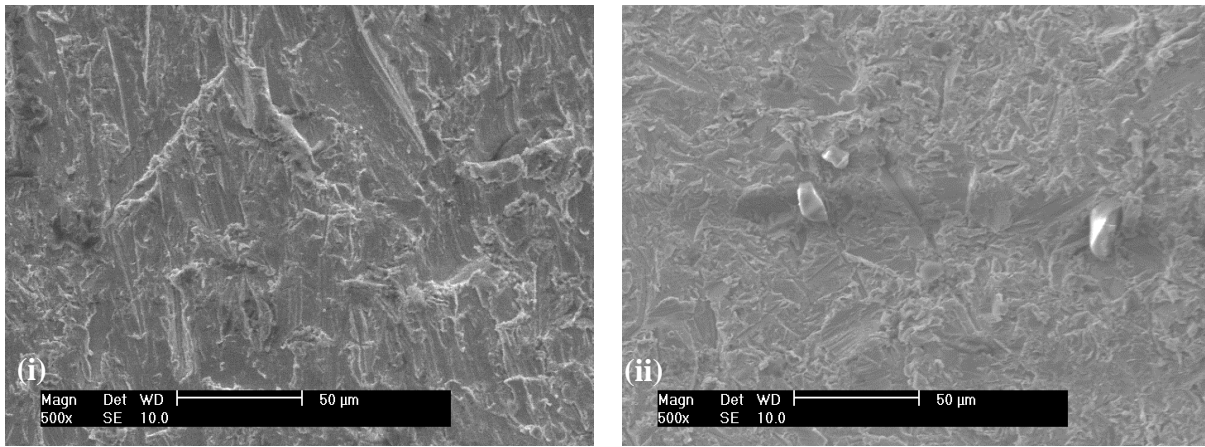


Figure 5 SEM images of cut face (i) SCR (ii) RCR

Tilting the cutting head by 12 degrees in the direction of jet traverse improved the visual quality of the cut. The DA at kerf exit was reduced from $22.0^{\circ} \pm 1.8$ to $13^{\circ} \pm 1.7$ for 26.9 mm thick specimens (figure 6).

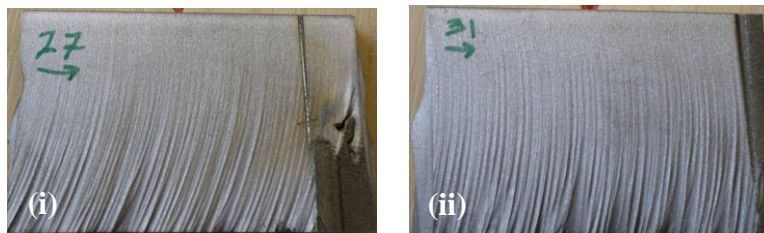


Figure 6 Modification of θ for 26.9 mm thick specimens (i) 90° (ii) 102°

Abrasive grit embedment was most evident in the IDR, as can be seen from the greater quantity of dark flecks at the top of the cut (figure 7(i)). The garnet particles fragmented during cutting producing smaller pieces with sharp edges to cut the material. Some of these fragments were observed in the RCR, most notably towards the exit region of the cut (figure 7(ii)). For this application, abrasive grit embedment is considered unimportant because subsequent processes remove up to 2 mm of material from the cut face.

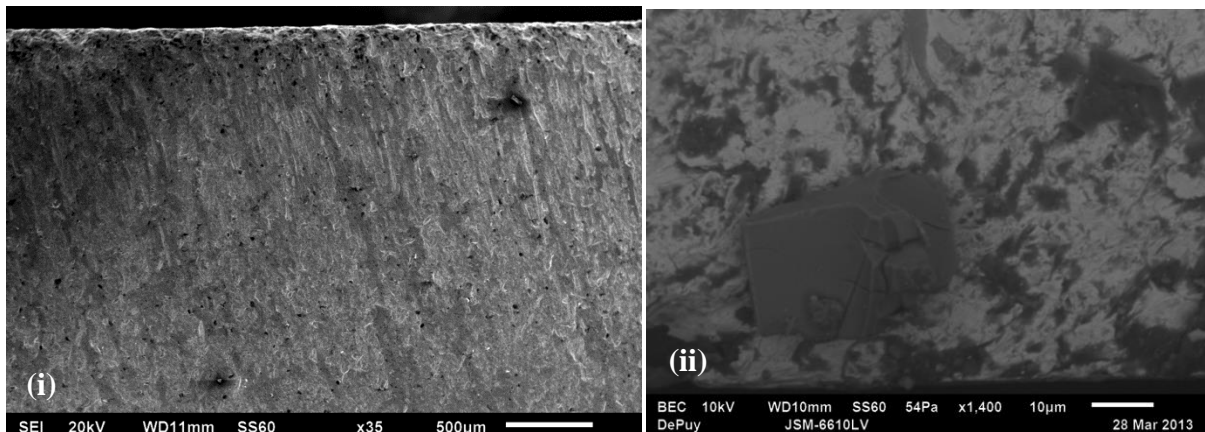


Figure 7 SEM images of abrasive embedment (i) Greater quantity of abrasive (dark flecks) in the IDR (ii) Garnet fragment embedded in RCR at kerf exit

Material removal during AWJC of ceramics and metals are characterised as brittle and ductile respectively. Ductility is the ability of a material to deform without fracture under an applied load and can be expressed by percentage elongation. High-strength metals normally have low ductility. CoCrMo has a low ductility of 11%, compared with that of stainless steel (12-40% for 316L) and mild steel (up to 50% for 304). Arola (1997) used the parameter of surface skewness to demonstrate the effect of ductility and corresponding critical strain for material removal. The surface skewness indicates the symmetry in amplitude distribution curve about a profile mean line. An increase in ductility was related to an increase in surface skewness. With respect to free abrasive erosion, metals with less resistance to abrasive penetration would be prone to exhibit a positively skewed (i.e. smoother) surface. Ti6Al4V and Molybdenum were shown to be negatively skewed. These two metals had significantly greater elastic moduli of the six metals tested. Pon Selvan and Raju (2011) used the elastic modulus as a parameter to calculate the depth of cut (D_c) for different materials. The model accurately predicted D_c for experimental cuts of CoCrMo at V_t 200 mm/min. However, at V_t 80 mm/min CoCrMo cut 55% deeper than the predictive model and at V_t 400 mm/min a 33% shallower cut was obtained.

Hard materials offer more resistance to abrasive wear. The abrasive must be significantly harder than the material to be cut as there is a linear relation between the H_v of an abrasive and the rate of erosion (Gent et al.). Garnet abrasive has a hardness of 1100-1300 H_v (7.5-8 Mohs). CoCrMo is a hard metal with a 310 H_v . Materials as hard as polycrystalline diamond (6000 H_v) have been cut with abrasive waterjet using diamond abrasive (10000 H_v) (Axinte et al.). In the same study alumina (Al_2O_3) and silicon carbide (SiC) were also investigated but the hardness of the diamond abrasives allowed for >200 times greater productivity to achieve an acceptable cut finish. Alumina is used as a blast media for surface finishing of medical devices. The abrasive is more expensive than garnet but may be suitable for this application as it has greater cutting ability due to its superior hardness of 2600 H_v (9 Mohs).

3.2 Process Parameters

Depth of cut increased with decreasing traverse speed. Figure 8 demonstrates cut depth increasing on 30 mm diameter cylinders with reducing V_t from 200-80 mm/min ($m_a=490g/min$).



Figure 8 Cylindrical cut face after varying V_t (i) 200 mm/min (ii) 140 mm/min (iii) 80 mm/min

Equivalent cutting depths were achieved with flat and cylindrical sections for the same process parameters (figure 9). However, the end of the flat section required finishing with EDM. When cutting flat sections at maximum speed, the traverse speed must be reduced at the end of the cut

to account for the lagging effect of the abrasive waterjet. Alternatively a second pass may be performed to finish the cut. The shape of cylindrical sections allows the traverse speed to be kept constant because the material thickness naturally reduces towards the end of the cut. This is despite the slight increase in distance from the nozzle to the specimen.

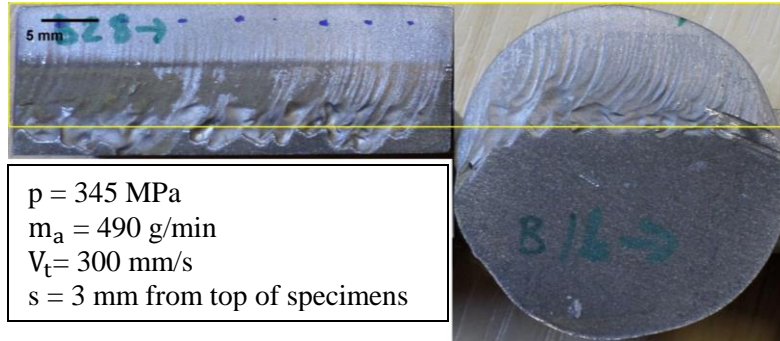


Figure 9 Flat and cylindrical sections after AWJC at 300 mm/min

To relate D_c and V_t for AWJC of CoCrMo, an empirical formula was experimentally derived from cutting cylinders of diameter 30 mm.. The jet impingement angle was set to 90° and the parallel standoff distance of 3 mm. Minimum cut depth was measured and a logarithmic equation fitted the dataset with $R^2=0.9747$ (figure 10). The equation can be used to estimate D_c for $p=345$ MPa and $m_a=490$ g/min at various traverse speeds (equation 1).

$$D_c = -14.72 \ln(V_t) + 92.798 \quad (1)$$

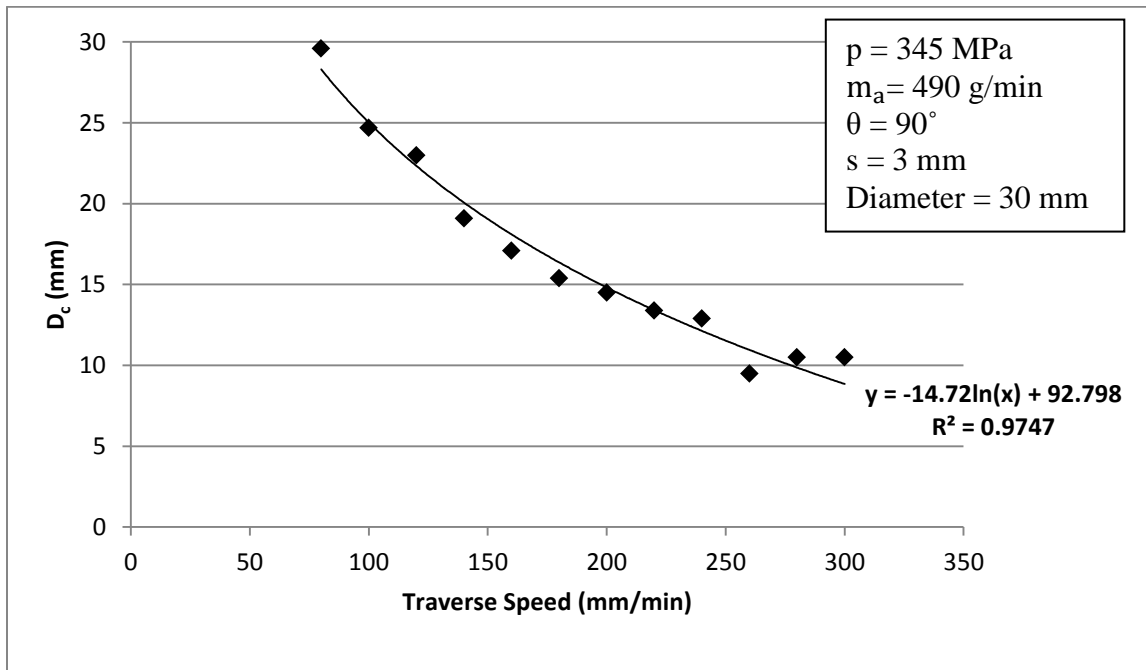


Figure 10 Effect of traverse speed on minimum cut depth of cylinders

Applying equation 1 to the 13 ± 1 mm samples, the predicted V_t is 226 ± 15 mm/min. This correlates well with the actual V_t that obtained a throughput, 220 mm/min (figure 14(ii)). The

equation may be modified to include a coefficient that modifies the limit traverse speed to the value assuring selected quality even on the worse part of the cutting wall, C_Q (Hlavac et al.). Re-writing the equation in terms of V_t :

$$V_t = C_Q \left[e^{\frac{D_c - 92.798}{-14.72}} \right] \quad (2)$$

Surface roughness is a useful parameter for interpreting the cut quality where striations are present. For most conditions, reducing V_t improves the surface roughness (figure 11). However, when attempting to maximize V_t , the region towards the bottom of the cut displayed low R_a values when approaching maximum V_t . A reduction of kinetic energy caused jet instability, turbulent flow and abrasive pooling. This resulted in superposition of large wavelength surface variations in this region, i.e. deep but smooth grooves with low R_a for the cut-off and traverse lengths used (figure 11). Approaching maximum V_t , R_a at the centre of the parts (just above the turbulent zone) remained high.

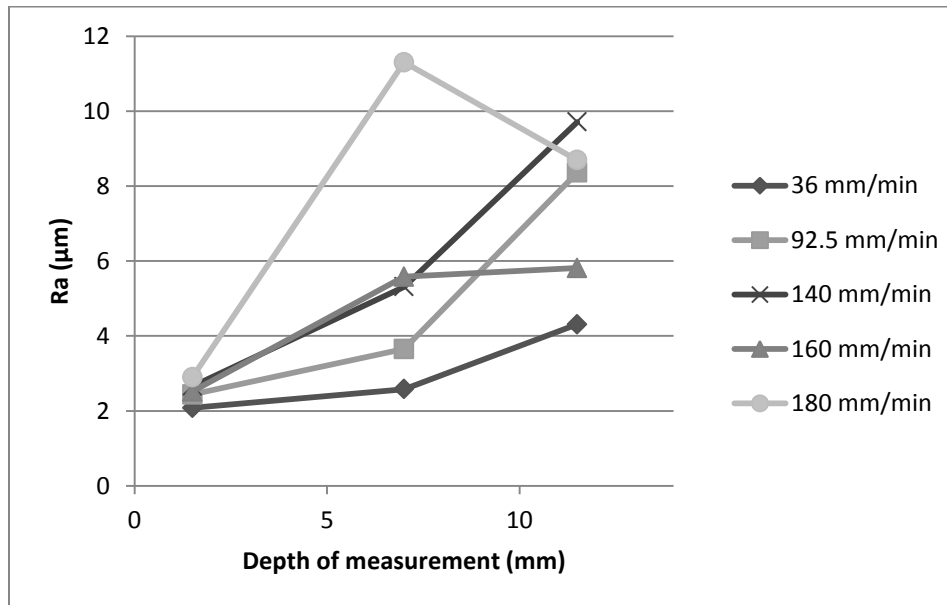


Figure 11 Effect of traverse speed on surface roughness ($m_a=300$ g/min)

Increasing m_a allows parts to be cut at a faster V_t but consumables cost increase. There is a point at which the higher abrasive costs offset the benefits of faster cutting. For these experiments, the optimum m_a was considered in terms of maximizing V_t rather than optimizing a cost-performance ratio. An upper limit of m_a 490 g/min was used for this nozzle combination because further increases would have led to abrasive build up in the delivery tube. Increasing m_a from 145 g/min to 300 g/min significantly improved the cut surface quality. The DA at kerf exit reduced by 10.3° and R_a reduced from 18 μm to 6.3 μm (figure 12).

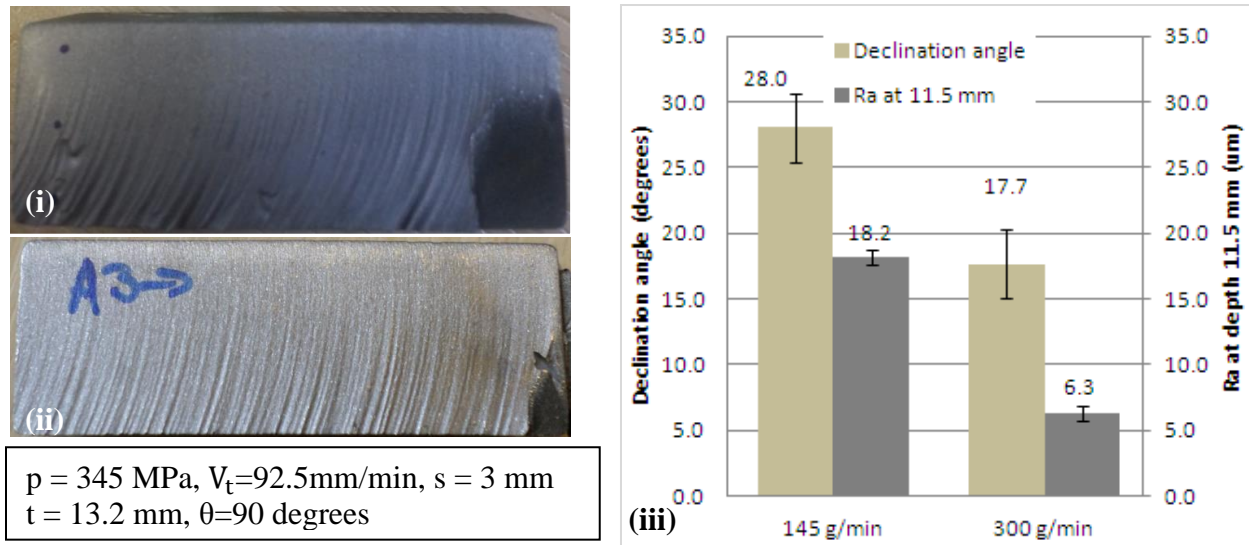


Figure 12 Influence of m_a on cut surface (i) $m_a = 145$ g/min, (ii) $m_a = 300$ g/min
(iii) Associated graph of DA and R_a

Figures 13 and 14 show the effect of m_a and V_t for parameters just above and below Through Cut (TC) requirements. The traverse speed required for TC of the 13 mm samples was 180 mm/min with m_a 300 g/min but increased to 220 mm/min with m_a 490 g/min.



Figure 13 Traverse speed (V_t) with $m_a = 300$ g/min (i) 160 mm/min (ii) 180 mm/min (TC) (iii) 200 mm/min (non-TC)



Figure 14 Traverse speed (V_t) with $m_a = 490$ g/min (i) 200 mm/min (ii) 220 mm/min (TC) (iii) 240 mm/min (non-TC)

3.3 AWJC of Investment Castings and Refractory Material

Ceramic shell materials include alumina, silica, and zircon. If still present at the cutting stage, the refractory is easily removed with AWJC by brittle fracture. Ceramic cores are sometimes used to reduce metal or to form intricate internal geometries. AWJC could cut through ceramic cores where necessary, although V_t adjustment may be required. The cost of disposal/reprocessing of the waste sludge containing ceramic, abrasive, metal particles and fragments requires consideration. For this application, due to the value of the metal fragments, sludge reprocessing results in a net gain. For AWJC systems with water recycling, water deionisation may be

required in addition to usual water filtration due to the presence of silica in refractory materials as pump performance may be adversely affected by dissolved silica.

The effect of a ceramic layer was investigated by fixing a 6 mm thick layer of aluminosilicate to the top surface of the flat 13 mm plate. Without a ceramic layer the flat specimens could be cut through with a maximum $V_t=220$ mm/min (figure 15(iii)), albeit with a significant degree of turbulence at the kerf exit. The ceramic-coated specimen with the same settings (except standoff set at 3 mm from top of ceramic surface) did not achieve a through cut (iv). A through cut was obtained at V_t 180 mm/min for the ceramic-coated plate. The increased turbulence at the bottom of the cut due to the ceramic layer can be observed in figure 15.

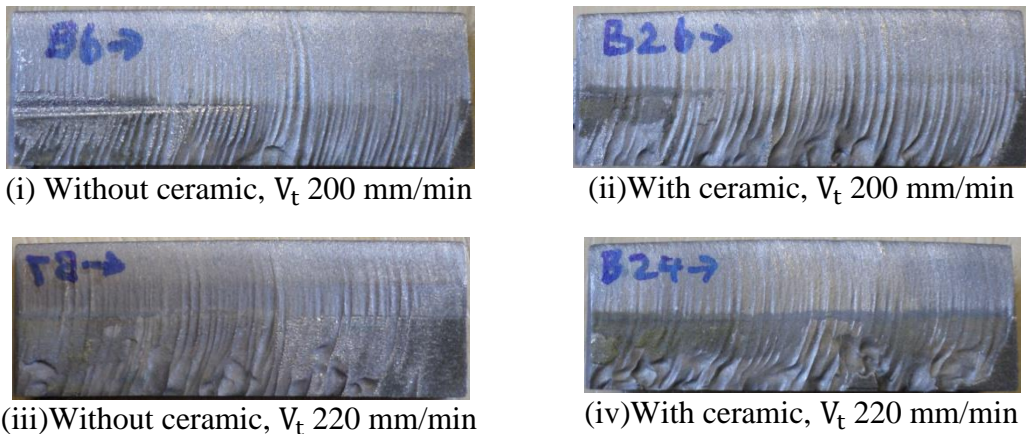


Figure 15 Effect of refractory layer fixed to the top surface

Increasing the standoff distance or modifying the shell removal process to remove more ceramic prior to cutting may be necessary to reduce the risk of nozzle collisions into refractory material on the casting surface. Standoff distance is far less influential than V_t , m_a or pressure on depth of cut (Pon Selvan and Raju). Increasing the standoff distance increases the diameter of the impinging jet. This results in increased rounding of the corner at the IDR as well as a change in the kerf shape and taper, due to loss in kinetic energy of the jet. Greater jet divergence whilst underwater cutting is expected to magnify the effect of standoff distance.

The cutting process must be flexible to account for casting defects that can be expected. Shrinkage porosity sometimes occurs in castings where there is a large cross-sectional area. These voids reduce the kinetic energy of the abrasive jet and increase the jet divergence and turbulence below the defect. Porosity was observed on three of the specimens cut with AWJC. A small degree of jet divergence was observed beneath the porosity but the reduction of jet energy was insignificant for the cutting depth of these specimens (figure 16).

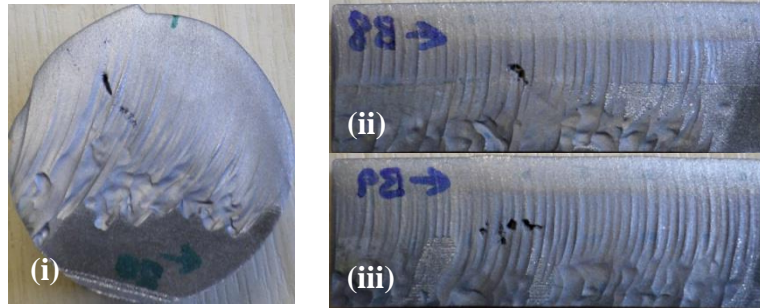


Figure 16 Effect of porosity on AWJC

3.4 Comparison of AWJC with alternative processes

Abrasive wheel and grinding are commonly used for cutting and finishing of investment castings. Abrasive wheel cutting is quick and efficient with relatively low machine footprint and is suitable for rough cutting of very thick metals and ceramics. The process leaves burrs which are removed by grinding or blasting with a hard abrasive media. Alumina, silicon carbide and CBN (Cubic Boron Nitride) are typical grinding belt abrasives. Grinding belt-life is significantly greater with automation because greater force can be applied to the parts than by manual grinding. The risk of personal injury and ergonomic impact are key concerns for manual grinding. Fixturing is critical for both processes due to the high forces involved. The processes generate significant heat at the interface, which may release residual stresses in the microstructure and reduce dimensional capability. AWJC requires minimal fixturing and there is no heat-affected zone. Depending on the quantity and complexity of grinding required, AWJC can compete with the processing time of abrasive wheel cutting and grinding for material thickness <20 mm.

Laser cutting is an alternative cutting process that is fast and efficient for flat plates. Solid-state (fiber) lasers are highly effective at cutting thin materials (<6 mm) and CO₂ lasers are used for thicker materials. A CrNi stainless steel (1.4301) of 10 mm thickness has been cut at 1000 mm/min with a 4 kW CO₂ laser and at 400 mm/min at 2 kW (Wandera, Kujanpaa and Salminen), significantly faster than the rate achieved with AWJC of CoCrMo. However, thick metals (>10 mm) are not normally processed by laser cutting due to the difficulty of achieving full melt ejection through the kerf. For thick-section laser cutting, a recast layer of dross remains on the underside of the cut. The thermal diffusivity of CoCrMo ($3.5 \times 10^{-6} \text{ m}^2/\text{s}$) (Miculescu et al.) is similar to that of the stainless steel alloy ($4 \times 10^{-6} \text{ m}^2/\text{s}$). Mild steel has a thermal diffusivity of $12 \times 10^{-6} \text{ m}^2/\text{s}$ and can be cut at much higher speeds. In contrast to AWJC, the size of the striations in laser cutting decrease with increase in traverse speed (due to excessive heat conduction). Yet insufficient power intensity limits the maximum traverse speed obtainable. The absorptivity, a key factor in laser cut quality, is dependent on the wavelength of laser radiation, angle of incidence, material type, as well as the temperature and phase of the metal. Maximizing power intensity requires accurate positioning of the focus point, which would require constant repositioning for cutting of thick solid cylinders. The laser assisting gas may be ineffective over the rounded surface. In addition, as laser cutting has primarily developed for flat sheet applications, cutting head geometries tend to be large, prohibiting their use for the majority of cast tree configurations.

Electrical discharge machining (EDM) is a highly accurate process whereby an electric current is used to erode away a conductive material. A charge is passed through a thin wire (approx 1 μ m thick) and the conductive material to be cut carries the other part of the charge. The apparatus is immersed in a dielectric liquid (usually deionised water). When the two charges get close, an electrical spark jumps the gap and the heat generated melts away tiny particles of the cut material. The process is suitable for intricate individual parts that require very tight tolerances (± 0.025 mm). Maximum V_t for a 13.6 mm CoCrMo plate was 3.5 mm/min, prohibitively slow and unsuitable for high-volume cutting applications. As runner system removal often occurs before complete refractory removal, a robust cutting process should be able to cope with some remaining ceramic material. EDM is unable to cut non-conductive materials and so could only be used after thorough refractory removal. Although non-conductive ceramics (zirconia and alumina) have recently been cut with EDM using an assisting electrode (Hösel, Müller and Reinecke), this approach would not be feasible for investment castings. One of the advantages of AWJC is that it can cut through combinations of different materials.

A thorough comparison of the cost of laser and AWJC has been conducted by (Zheng et al.). An approximate comparison of the three alternative cutting processes is given in table 4. Given that castings normally have thick, solid round gates and a degree of ceramic normally remains prior to cutting, laser cutting and EDM are presented with technical challenges and are currently unsuitable alternatives to the current abrasive wheel cutting and grinding process.

Table 4 Approx. cutting speeds and costs for selected cutting processes

	V_t for 13 mm thick plate	Equipment Cost (\$)	Running Cost (\$/hr)
AWJC	200 mm/min	450,000	70
Laser cutting	400 mm/min	800,000	55
EDM	3.5 mm/min	300,000	2

4. CONCLUSIONS

An empirical formula was generated to estimate D_c for varying V_t for high strength CoCrMo investment castings. For the same process conditions, flat plates and cylinders achieved an equivalent cut depth up to the end of the cut. Cylindrical gates are ideal for AWJC as they do not require V_t reduction towards end of cut to account for waterjet lag effect. The mechanism of material removal is similar to that of stainless steel and occurs via microchip formation, ploughing and rubbing.

The technical feasibility and cost considerations of alternative cutting methods for runner system removal for investment castings were discussed (abrasive wheel and grinding, laser cutting and EDM). Manual grinding processes carry risk of personal injury and ergonomic concerns. Laser cutting is unsuitable for cylindrical gates and EDM is prohibitively slow. Both would require thorough refractory removal prior to cutting. AWJC may be suitable for this process, primarily

depending on the casting tree configuration and gate thickness. Future research will include refinement and verification of the empirical formula for D_c to include the effect of pressure and alternative abrasives. Underwater cutting will be investigated as a means to reduce the noise level.

ACKNOWLEDGEMENTS

The authors would like to acknowledge the EU for the funding support under the Marie Curie Actions – Industry Academia Partnerships and Pathways, within Framework 7, Grant Agreement 251269, “MEDCAST”, and also for the funding support for FP7 “ConforM-Jet”.

REFERENCES

- Arola, D. and Ramulu, M. "Material Removal in Abrasive Waterjet Machining of Metals; Surface Integrity and Texture." *Wear* 210 (1997): 50-58. Print.
- ASTM. "Astm F75, Standard Specification for Cobalt-28 Chromium-6 Molybdenum Casting Alloy and Cast Products for Surgical Implants (Uns R30075)." 1998. Print.
- Axinte, D. A., et al. "Abrasive Waterjet Cutting of Polycrystalline Diamond: A Preliminary Investigation." *International Journal of Machine Tools and Manufacture* 49.10 (2009): 797-803. Print.
- Cawley, J., et al. "A Tribological Study of Cobalt Chromium Molybdenum Alloys Used in Metal-on-Metal Resurfacing Hip Arthroplasty." *Wear* 255.7–12 (2003): 999-1006. Print.
- Gent, M., et al. "Experimental Evaluation of the Physical Properties Required of Abrasives for Optimizing Waterjet Cutting of Ductile Materials." *Wear* 284–285.0 (2012): 43-51. Print.
- Hlavac, L. M., et al. "Experimental Method for the Investigation of the Abrasive Water Jet Cutting Quality." *Journal of Materials Processing Technology* 209.20 (2009): 6190-95. Print.
- Hösel, T., C. Müller, and H. Reinecke. "Spark Erosive Structuring of Electrically Nonconductive Zirconia with an Assisting Electrode." *CIRP Journal of Manufacturing Science and Technology* 4.4 (2011): 357-61. Print.
- Miculescu, M., et al. "Thermal Diffusivity of Materials Using Flash Method Applied on CoCr Alloys." *UPB Scientific Bulletin* 70.2 (2008): 71-81. Print.
- Pon Selvan, M.C. , and N. M. Raju. "An Experimental Investigation on Depth of Cut in Abrasive Waterjet Cutting of Aluminium." *International Journal of Engineering Science and Technology (IJEST)* 3.4 (2011): 2950-54. Print.
- Wandera, C., V. Kujanpaa, and A. Salminen. "Laser Power Requirement for Cutting Thick-Section Steel and Effects of Processing Parameters on Mild Steel Cut Quality." *Proceedings of the Institution of Mechanical Engineers Part B-Journal of Engineering Manufacture* 225.B5 (2011): 651-61. Print.
- Zheng, H. Y., et al. "Quality and Cost Comparisons between Laser and Waterjet Cutting." *Journal of Materials Processing Technology* 62.4 (1996): 294-98. Print.

NOMENCLATURE

C_Q = Coefficient that modifies the limit traverse speed to the value assuring selected quality even on the worse part of the cutting wall

D_c = Depth of cut (mm)

H_v = Hardness (Vickers)

m_a = Mass flow rate of abrasive particles (g/min)

p = water pressure (MPa)

R_a = surface roughness average (μm)

s = standoff distance (mm)

t = material thickness (mm)

V_t = Traverse speed (mm/min)

θ = Jet impingement angle ($^\circ$)

AWJC = Abrasive Water Jet Cutting

DA = Declination Angle, i.e. the angle between the tangent to the striation curve and the impinging jet axis ($^\circ$)

EDM = Electrical Discharge Machining

IDR = Initial Damage Region

SCR = Smooth Cut Region

SEM = Scanning Electron Microscopy

RCR = Rough Cut Region

TC = Through Cut